ACCP
American College of Clinical Pharmacology
Advancing Clinical Care through Pharmacology®

Original Article

Pharmacokinetic Modeling of Ketamine Enantiomers and Their Metabolites After Administration of Prolonged-Release Ketamine With Emphasis on 2,6-Hydroxynorketamines

Clinical Pharmacology in Drug Development
2022, 11(2) 194–206

DOI: 10.1002/cpdd.993

Michael Weiss[1] and Werner Siegmund[2]

Abstract

Modeling of metabolite kinetics after oral administration of ketamine is of special interest because of the higher concentrations of active metabolites because of the hepatic first-pass effect. This holds especially in view of the potential analgesic and antidepressant effects of 2R,6R- and 2S,6S-hydroxynorketamine at low doses of ketamine. Therefore, a 9-compartment model was developed to analyze the pharmacokinetics of ketamine enantiomers and their metabolites after racemic ketamine administered intravenously (5 mg) and as 4 doses (10, 20, 40, and 80 mg) of a prolonged-release formulation (PR-ketamine). Using a population approach, the serum concentration-time data of the enantiomers of ketamine, norketamine, dehydronorketamine, and 2,6-hydroxynorketamine obtained in 15 healthy volunteers could be adequately fitted. The estimated model parameters were used to simulate serum concentration-time profiles; after multiple dosing of PR-ketamine (2 daily doses of 20 mg), the steady-state concentrations of R- and S-ketamine were 1.4 and 1.3 ng/mL, respectively. The steady-state concentration of 2R,6R-hydroxynorketamine exceeded those of R-norketamine (4-fold), R-dehydonorketamine (8-fold), and R-ketamine (46-fold), whereas that of 2S,6S-hydroxynorketamine exceeded that of S-ketamine by 14-fold. The model may be useful for identifying dosing regimens aiming at optimal plasma concentrations of 2,6-hydroxynorketamines.

Keywords

chiral metabolism, ketamine, pharmacokinetic modeling, prolonged release

Racemic ketamine is a mixture of equal amounts of S- and R-enantiomers (R-K, S-K). In patients, the parent drug exerts the major anesthetic/analgesic effect but also significant dissociative/hallucinogenic side effects by antagonism of the N-methyl-D-aspartate (NMDA) receptor. Ketamine is nearly completely oxidized by N-demethylation to the less active primary metabolite norketamine, which secondarily undergoes oxidative dehydrogenation to the inactive dehydronorketamine (R-DHNK, S-DHNK) and hydroxylation to 12 steric forms of hydroxynorketamine, of which the 2R,6R- (R-HNK) and 2S,6S- (S-HNK) stereoisomers lack the undesired dissociative/hallucinogenic effects of the parent ketamines and the NKs.[1–3] The HNKs can also be slowly formed by primary hydroxylation followed by demethylation.[1] In contrast to ketamine and NK, HNKs exert antidepressant-related effects, analgesic properties, and relief of allodynia in experimental studies in rodents.[4,5] These effects are independent of the NMDA-receptor antagonism and are most likely

[1]Department of Pharmacology, Martin Luther University Halle-Wittenberg, Halle, Germany
[2]Department of Clinical Pharmacology, Center of Drug Absorption and Transport (C_DAT), University Medicine Greifswald, Greifswald, Germany

Submitted for publication 27 April 2021; accepted 30 May 2021.

Corresponding Author:
Michael Weiss, PhD, Department of Pharmacology, Martin Luther University Halle-Wittenberg, Halle 06097, Germany
(e-mail: michael.weiss@medizin.uni-halle.de)

caused by binding to α-amino-3-hydroxy-5-methyl-4-isoxazole-propionic acid glutamate receptors and the α7-acetylcholine receptor and modulation of synaptic pathways in brain tissues that are involved in the pathogenesis of neuropathologic disorders.[2,3] Therefore, the HNKs are still the subject of ongoing experimental and clinical reevaluations and are discussed in a lively manner in light of new clinical applications in treatment of patients with drug-resistant depression and neuropathic pain.[6–8]

There is evidence that after oral administration of racemic ketamine, a substantial amount of the 2,6-HNKs is formed by hepatic first-pass metabolism.[9] In a recently performed noncompartmental pharmacokinetic study (NCA) of a new prolonged-release ketamine tablet (PR-ketamine) in healthy human subjects, we have shown that the total plasma exposure (area under the curve [$AUC_{0-\infty}$]) of R- and S-HNK is about 20 times (S-form) to 40 times (R-form) that of the respective ketamine-enantiomer and that the exposure to R-HNK is more than 2-fold higher than that to S-HNK.[10] However, these observed differences in AUCs could not be explained by NCA, because it is impossible to estimate pharmacokinetic parameters of the metabolites with this method (except for renal clearances). Therefore, we reanalyzed the data using a pharmacokinetic model to get information about presystemic and systemic formation of the primary and secondary metabolites and the elimination clearance of the DHNK and HNK stereoisomers. The model and estimated parameters also allowed the prediction of serum concentration-time profiles of ketamine and all metabolites after multiple-dose administration. Because PR-ketamine might be an efficient and safer pharmaceutical dosage form for treatment of depression and neuropathic pain, the selection of dosage regimens, especially with respect to the 2,6-HNKs, appears to be of clinical relevance.

An essential part of analyzing the prolonged-release kinetics of PR-ketamine was the selection of an appropriate empirical absorption model.[11] Fitting the serum concentration-time data of ketamine and NK after oral administration of ketamine allowed discriminating between fraction absorbed and hepatic extraction as determinants of ketamine bioavailability. Together with the model parameters obtained in the same subjects after intravenous dosing, all model parameters of both stereoisomers of ketamine and their metabolites could be estimated with acceptable precision. Earlier approaches to pharmacokinetic modeling of chiral ketamine metabolism were limited in so far as they only concerned intravenous administration[12,13] or oral dosing of S-ketamine, not including secondary metabolites.[14,15]

Methods

Clinical Study Data

The study was performed in 15 healthy white German subjects (10 men, 5 women; aged 20-35 years; body mass index, 19.4-27.6 kg/m^2). The details of the study, including the ethical committee's approval and the analytical methods, have been reported elsewhere.[10] In a controlled, open label, consecutive, single-dose 5-period study with at least a 7-day washout between study periods, the pharmacokinetics of ketamine and its metabolites were evaluated under fasting conditions after oral administration of 10, 20, 40, and 80 mg PR-ketamine (Develco Pharma, Schopfheim, Germany, U.S. Patent No. 10,335,379;2019) and after intravenous infusion of 5 mg ketamine hydrochloride in 250 mL of saline within 30 minutes (Ratiopharm, Ulm, Germany). Venous blood was collected via an indwelling forearm cannula before beginning the intravenous infusion of ketamine and after 10, 20, 30, 40, and 50 minutes and 1, 1.5, 2, 3, 4, 6, 8, 12, and 24 hours. In case of PR-ketamine, blood was sampled via the indwelling cannula before and after 0.5, 1, 1.5, 2, 2.5, 3, 3.5, 4, 4.5, 5, 6, 7, 8, 12, 16, and 24 hours and after 36, 48, and 60 hours by repeated venipuncture. The quantitative analysis of ketamine and its metabolites in serum and urine was performed using a validated liquid chromatography-tandem mass spectrometry method.[16,17]

Pharmacokinetic Model

The structure of the compartmental model used in this study is shown in Figure 1. It represents the simplest possible model for analyzing the following processes: first, the input and disposition of R- and S-ketamine; second, the metabolism to the primary metabolites R-NK and S-NK; third, the further transformation to the secondary metabolites R-DHNK and S-DHNK as well as to R-HNK and S-HNK. A 3-compartment model was used for ketamine disposition, whereas a 2-compartment model proved optimal for NK, HNK, and DHNK. Note that the rate constant (k_t) in the intermediate compartments accounts for the hepatic transit time of the generated norketamine.[18] After oral administration, the bioavailability F of ketamine is determined by the fraction absorbed, F_a, and hepatic extraction, E_{hK}: $F = F_a(1 - E_{hK})$. This relationship is based on the assumption that the contribution of the gut wall to the formation of NK can be neglected.[15] The amounts of NK, HNK, and DHNK that are generated by hepatic first-pass metabolism are given as fraction of dose by $h_{NK}F_aE_{hK}F_{hNK}$, $F_aE_{NK\text{-}HNK}$, and $F_aE_{NK\text{-}DHNK}$, respectively, where h_{NK} denotes the fraction of hepatic clearance that generates NK.[19]

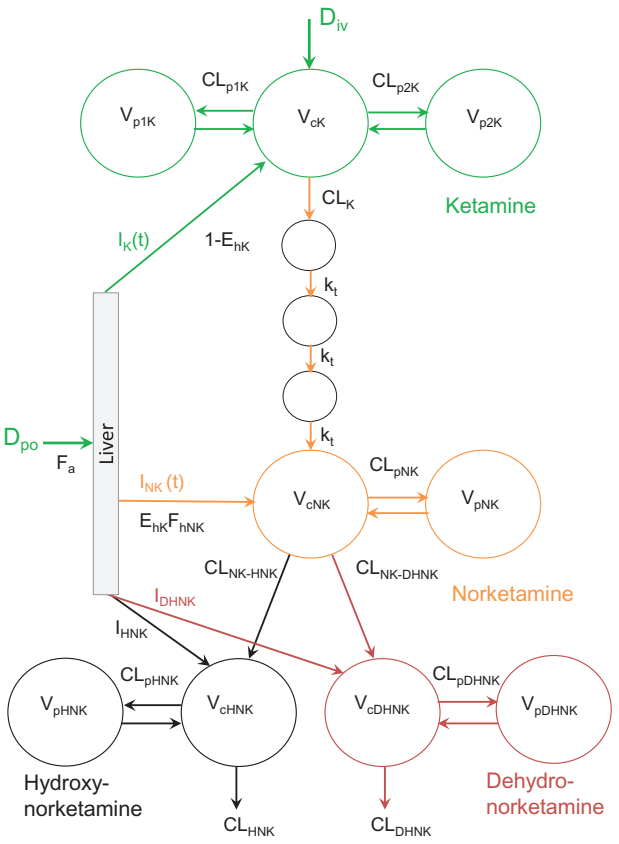

Figure 1. Pharmacokinetic model of ketamine (K) metabolism to norketamine (NK), 2,6-hydroxynorketamine (HNK), and dehydronorketamine (DHNK) after intravenous (D_{iv}) and oral (D_{po}) administration. V_{*K}, CL_{p*K}, and CL_K denote the distribution volume, distribution clearance, and metabolic clearance of ketamine. The delay in the generation of NK is modeled by a chain of 3 compartments with time constants (k_t). V_{*NK}, CL_{pNK}, $CL_{NK\text{-}HNK}$, and $CL_{NK\text{-}DHNK}$ denote the distribution volume, distribution clearance, and clearance of NK that forms HNK and DHNK, respectively. V_{*HNK}, CL_{p*HNK}, CL_{HNK}, and V_{*DHNK}, CL_{p*DHNK}, CL_{DHNK} are the distribution volume, distribution clearance, and elimination clearance of HNK and DHNK, respectively. F_a and E_{hK} denote the fraction absorbed and hepatic extraction of ketamine. F_{hNK} is the hepatic availability of generated NK; $I_K(t)$ and $I_{NK}(t)$ are input functions defined by equations 1, 2, and 4. The input functions of secondary metabolites $I_{HNK}(t)$ and $I_{DHNK}(t)$ are characterized by their first-pass generation, that is, extraction ratios $E_{K\text{-}HNK}$ and $E_{K\text{-}DHNK}$.

Note that $F_{hNK} = 1 - E_{NK\text{-}HNK} - E_{NK\text{-}DHNK}$ is the fraction of NK formed in the liver that survives a single passage through the liver. Because h_{nk} is >0.8,[15] we assume $h_{nk} = 1$, as in most previous approaches of modeling of ketamine pharmacokinetics.[12–15]

An important feature of the model is the evaluation of the time course of absorption rate, that is, the rate of ketamine input into the central compartment, I(t), after oral administration of PR-ketamine. Using a sum of inverse Gaussian density functions (IGs) as a model of absorption (or input) rate[11,20,21]:

$$I_K(t) = DF(pf_{1K}(t) + (1-p)f_{2K}(t)) \quad (1)$$

where D is dose and $f_i(t)$ denotes the ith IG[22]:

$$f_i(t) = \sqrt{\frac{MT_i}{2\pi\, RD_i^2\, t^3}} \exp\left[-\frac{(t-MT_i)^2}{2\, RD_i^2\, MT_i t}\right] \quad (2)$$

where MT_i and RD^2 are the scale and shape parameters, respectively, of the ith IG function. The mean input time (MIT_K) is then obtained as

$$MIT_K = p_K MT_{1K} + (1-p_K)MT_{2K} \quad (3)$$

The first-pass formation rate of NK is given by

$$I_{NK}(t) = DF_a E_{hK}(1 - E_{NK-HNK} - E_{NK-DHNK}) \times (pf_{1NK}(t) + (1-p)f_{2NK}(t)) \quad (4)$$

and the mean input time of NK is

$$MIT_{NK} = p_{NK} MT_{1NK} + (1-p_{NK})MT_{2NK} \quad (5)$$

For the first-pass input rates I_{HNK} and I_{DHNK}, the same time function (equation 4) was used, but with the amounts $DF_aE_{NK\text{-}HNK}$ and $DF_aE_{NK\text{-}DHNK}$ assuming that first-pass formation of HNK and DHNK occurs via NK.

Data Analysis After Intravenous Infusion

A population approach (nonlinear mixed-effects modeling) with maximum likelihood estimation via the EM (MLEM) algorithm implemented in ADAPT software (version 5) was used for data analysis.[23] The MLEM program provides estimates of population mean and intersubject variability as well as of individual subject parameters (conditional means). We assumed that the estimated parameters followed a multivariate lognormal distribution and that the residual error was normally distributed with a standard deviation that was a linear function of the measured quantity C_i:

$$VAR_i = [s_0 + s_1 C(t_i)]^2 \quad (6)$$

Goodness of fit was assessed using the Akaike information criterion (AIC) and by plotting the predicted versus the measured responses.

The stepwise fitting procedure was as follows. After fitting the ketamine data after intravenous infusion using a 3-compartment model (Figure 1), the individual parameter estimates (conditional means) were fixed when fitting the NK data, the only adjustable parameters remaining are k_t, V_{cNK}, V_{pNK}, CL_{pNK}, and CL_{NK}.

As shown in Figure 1, it was assumed that elimination occurs solely by metabolism to NK (CL_{NK}). Then, when fitting HNK and DHNK data obtained after the intravenous dosing simultaneously, the estimates of CL_K, V_{cK}, V_{p1K}, V_{p2K}, CL_{p1K}, CL_{p2K}, k_t, V_{cNK}, V_{pNK}, CL_{pNK}, and CL_{NK} were held fixed, and the adjustable free parameters were the disposition parameters of the metabolites. Thereby, we assumed that $CL_{NK\text{-}DHNK} = CL_{NK} - CL_{NK\text{-}HNK}$. Here, an identifiability problem arises: one has to make an a priori assumption about the relative sizes of HNK and DHNK formation clearances; we started with $CL_{NK\text{-}HNK}$ of approximately 0.7 $CL_{NK\text{-}DHNK}$[13] as an initial estimate of $CL_{NK\text{-}HNK}$ in the fitting procedure. After testing different initial estimates for the other parameters, we selected the result with the lowest AIC.

Data Analysis After Oral Administration of PR-Ketamine

In fitting the serum concentration-time data after oral administration of PR-ketamine, all parameters estimated from intravenous data (as described above) were held fixed. We explored 2 alternative models that differed in the a priori assumptions concerning the first-pass generation of HNK and DHNK.

Scenario 1: Bioavailability F estimated by fitting the ketamine data was fixed when fitting the NK data to estimate the apparent extraction ratio $E_{hK,app} = E_{hK}F_{hNK}$ with $F_{hNK} = 1 - E_{NK\text{-}HNK} - E_{NK\text{-}DHNK}$; the subscripts denote the generation of HNK and DHNK from the NK during hepatic first-pass (compare equation 4). Then, by adding the first-pass input terms $I_{HNK}(t)$ and $I_{DHNK}(t)$ in the model used to fit the intravenous data (Figure 1), the first-pass extraction values $E_{NK\text{-}HNK}$ and $E_{NK\text{-}DHNK}$ together with the input time parameters were estimated by fitting the oral HNK and DHNK data simultaneously. This allowed the calculation of the real values of hepatic extraction E_{hK} (from the estimates of $E_{hK,app}$ and F_{hNK}) and absorbed fraction ($F_a = F/(1 - E_{hK})$).

Scenario 2: Assuming that the first-pass generation of HNK and DHNK occurs from ketamine via intermediate steps to form the amounts $DF_aE_{K\text{-}HNK}$ and $DF_aE_{K\text{-}DHNK}$, the extraction ratios $E_{K\text{-}HNK}$ and $E_{K\text{-}DHNK}$ were estimated as described above but with the uncorrected values for F_a and E_{hK} derived from the NK fit (ie, $F_{hNK} = 1$).

Simulation

For the simulation of serum concentration-time profiles after multiple oral doses of PR-ketamine using the SIM module of ADAPT5,[23] we implemented the FORTRAN code program for an IG input function and multiple dosing recently developed by David D'Argenio (personal communication). Concentration-time profiles of ketamine enantiomers and their metabolites NK, DHNK, and HNK were simulated using the estimated population mean values. Based on the dosage to reach a therapeutic concentration of R-HNK suggested on the basis of AUC data,[10] we simulated concentration profiles for a daily PR-ketamine dose of 40 mg (12 hourly doses of 20 mg). Furthermore, we simulated the response to an infusion of 35 mg (R,S)-ketamine over 40 minutes, as previously used in pharmacodynamic studies.[12,24,25] Monte Carlo simulations ($n = 1000$) were performed to provide insight into the effect of intersubject variability on the simulated curves. Thus, the 90% prediction interval for the R-HNK concentration was calculated from the 5th and 95th percentiles of the simulated population.

Statistical Methods

The individual parameter estimates (conditional means of the MLEM algorithm) were used in statistical analysis. The Wilcoxon signed rank test was performed to evaluate differences in the parameters reported in Table 1. Friedman nonparametric repeated-measures analysis of variance tests with Dunn's multiple-comparison posttests were used to analyze the results obtained for the 4 doses after oral administration (Table 2). The S-plus and SPSS packages were used for data analysis.

Results

The pharmacokinetic model as shown in Figure 1 fitted the serum concentration-time profiles of R-ketamine and S-ketamine and their downstream metabolites well. This will be illustrated here for the R-enantiomer. All 40 goodness-of-fit plots are depicted in the Supplemental materials together with plots of model-predicted average concentration-time curves (simulated using the mean parameter estimates) and medians of the observed data for R-ketamine and metabolites. The disposition of R- and S-ketamine was best described by a 3-compartment model, whereas for the metabolites a 2-compartment model was found optimal by the AIC criterion. The simultaneous fit to R-HKN and R-DHKN data after intravenous infusion is demonstrated in Figure 2 by the plotting of model-predicted concentration-time curves together with the medians of the observed data. For PR-ketamine, the fits of the ketamine and NK data showed that the double IG function (equation 1) is an appropriate input function. Illustrating the interindividual variability of bioavailability, Figure 3 (upper) presents the fits of PR-ketamine data for 3 subjects characterized by the highest, middle, and lowest C_{max} values, with F values of 8%, 11%, and 34%. Figure 3 (bottom) shows the

Table 1. Pharmacokinetic Parameters of Ketamine Hydrochloride After Intravenous Infusion of 5 mg/30 minutes in 15 Healthy Human Subjects

	Symbol (Unit)		R-Enantiomer	S-Enantiomer
Ketamine (K)				
Clearance	CL_K	(L/h)	86.5 (18)	89.5 (21)
Volume central compartment	V_{cK}	L	65.0 (41)	69.0 (44)
Intercompartmental clearance 1	CL_{p1K}	L/h	29.7 (32)	28.5 (51)
Volume peripheral compartment 1	V_{p1K}	L	202 (83)	291 (94)
Intercompartmental clearance 2	CL_{p2K}	L/h	208 (29)	210 (24)
Volume peripheral compartment 2	V_{p2K}	L	119 (32)	137 (22)
Volume at steady state	V_{ss}	L	386 (56)	497 (60)
Residual variability[a]	σ_0		0.016	0.0006
	σ_1		0.103	0.106
Norketamine (NK)				
Clearance	CL_{NK}	L/h	61.5 (25)	40.3 (39)[b]
Volume central compartment	V_{cK}	L	69 (31)	52 (58)
Intercompartmental clearance	CL_{pNK}	L/h	67.5 (27)	47.6 (31)[b]
Volume peripheral compartment	V_{pNK}	L	161 (21)	129 (38)
Hepatic formation transit time	MTT_{NK}	Min	5.78 (47)	5.46 (38)
Residual variability[a]	σ_0		0.109	0.109
	σ_1		0.060	0.060
Hydroxynorketamine (HNK)				
Formation clearance	$CL_{NK\text{-}HNK}$	L/h	22.6 (25)	18.9 (35)
Clearance	CL_{HNK}	L/h	7.2 (37)	23.6 (43)[c]
Volume central compartment	V_{cHNK}	L	9.7 (28)	12.7 (80)
Intercompartmental clearance	CL_{pHNK}	L/h	41.3 (53)	34.4 (71)
Volume peripheral compartment	V_{pHNK}	L	80.0 (21)	39.9 (76)
Residual variability[a]	σ_0		0.096	0.08
	σ_1		0.023	0.001
Dehydronorketamine (DHNK)				
Formation clearance	$CL_{NK\text{-}DHNK}$	L/h	24.3 (27)[d]	40.7 (14)[c]
Clearance	CL_{DHNK}	L/h	115 (20)	116 (15)
Volume central compartment	V_{cDHNK}	L	33.4 (38)	25.7 (50)
Intercompartmental clearance	CL_{pDHNK}	L/h	141 (62)	155 (57)
Volume peripheral compartment	V_{pDHNK}	L	7.6 (113)	73.5 (143)
Residual variability[a]	σ_0		0.216	0.238
	σ_1		0.075	0.114

Population means with intersubject variability (expressed as %CV) in parentheses.
[a] σ_0, σ_1, residual variability (variance of the measurement error: $VAR_i = [\sigma_0 + \sigma_1 C(t_i)]^2$).
[b] $P < .01$ compared with R-enantiomer.
[c] $P < .001$ compared with R-antiomer.
[d] $P < .001$ compared with HNK.

R-NK fits for the same subjects. Note that because of the higher hepatic extraction ratio (E_{Kh}) of 0.99 for the subject with the lowest F, the generated R-NK concentration is not much different from that of the subject with F = 11% ($E_{Kh} = 0.89$). Figure 4 displays the simultaneous fit to the R-HNK and R-DHNK data after administration of a 40-mg PR-ketamine tablet with predicted population mean curves (with open squares representing the mean values of HNK data and open circles those of DHNK data). Table 1 lists the population mean estimates of the parameters together with their intersubject variability obtained after intravenous infusion of ketamine. Although there were no significant differences in the disposition kinetics between R-and S-ketamine, the clearance of R-NK (61.5 L/h) significantly exceeded that of S-NK (40.4 L/h), $P < .01$). Importantly, the a priori assumption of $CL_{NK\text{-}HNK} > CL_{NK\text{-}DHNK}$[13] did not lead to a reasonable fit. The best result was obtained with $CL_{NK\text{-}HNK} \sim CL_{NK\text{-}DHNK}$ for the R-stereoisomers. The formation clearance for S-DHNK (40.7 L/h) was significantly higher than that of R-DHNK (24.3 L/h), $P < .001$, whereas the formation clearance $CL_{NK\text{-}DHNK}$ of S-DHNK (40.7 L/h) exceeded that of R-DHNK (24.3 L/h), $P < .001$. Most interestingly, however, the elimination clearance of both R- and S-DHNK was

Table 2. Pharmacokinetic Parameters for 4 Doses of Prolonged-Release Ketamine

	Symbol	Isomer	10 mg	20 mg	40 mg	80 mg
Bioavailability of ketamine	F (%)	R	13.2 (48)	12.4 (55)	15.3 (55)	13.5 (47)
		S	13.4 (68)	12.1 (72)	14.6 (57)	13.4 (49)
Fraction absorbed of ketamine	F_a (%)	R	88.9 (17)	97.3 (6)	95.3 (9)	91.2 (15)
		S	73.6 (38)	74.1 (32)[a]	85.3 (18)[d]	60.6 (34)[a,e]
Hepatic first-pass extraction of ketamine	E_{hK} (%)	R	83.2	84.9	81.5	83.5
		S	77.9	78.2	80.1	75.3
Hepatic first-pass extraction of generated NK that forms HNK	$E_{K\text{-}HNK}$ (%)	R	7.59 (153)	2.75 (147)	2.31 (177)	0.87 (158)[c]
		S	13.1 (248)	9.74 (212)[a]	12.9 (143)[a]	14.6 (121)[b]
Hepatic first-pass extraction of generated NK that forms DHNK	$E_{K\text{-}DHNK}$ (%)	R	23.6 (106)	23.2 (81)	3.84 (117)[c,d]	10.6 (44)
		S	42.9 (113)	16.1 (156)	10.7 (66)	1.08 (196)[a,c]
Mean input time of ketamine	MIT_K (h)	R	8.17 (33)	6.34 (11)	8.10 (16)	7.73 (13)
		S	10.4 (47)	6.23 (19)	7.51 (21)	8.18 (22)
Mean input time of norketamine	MIT_{NK} (h)	R	6.45 (21)	7.06 (27)	8.45 (27)	9.45 (13)
		S	8.66 (59)	8.38 (38)	7.59 (19)	9.29 (31)

Population means with intersubject variability (expressed as %CV) in parentheses.
[a] $P < .05$ compared with R-enantiomer.
[b] $P < .001$ compared with R-enantiomer.
[c] $P < .01$ compared with 10-mg dose.
[d] $P < .01$ compared with 20-mg dose.
[e] $P < .01$ compared with 40-mg dose.

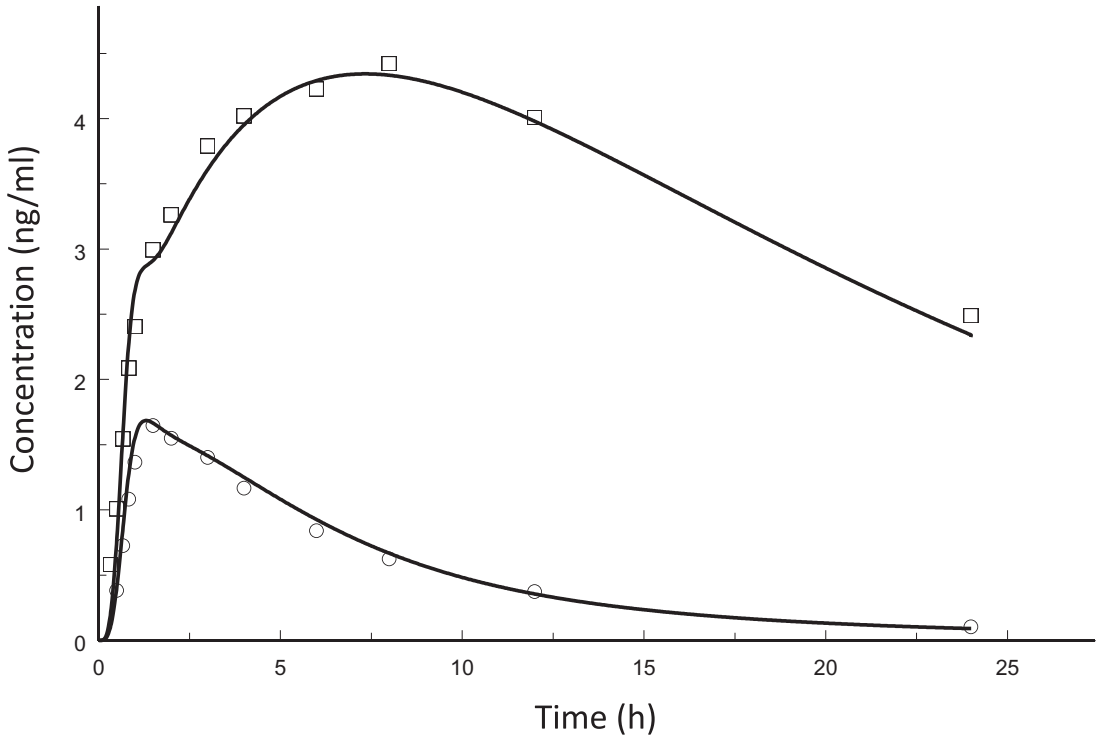

Figure 2. Model-predicted average concentration-time curves for 2R,6R-hydroxynorketamine (R-HNK) and R-dehydronorketamine (R-DHNK) after intravenous administration of 5 mg R/S-ketamine, with the medians of the R-HNK data (open squares) and R-DHNK data (open circles). The curves were simulated using the population mean parameter estimates (Table 1).

more than 6 times higher than that of R-and S-HNK ($P < .001$), and the clearance of S-HNK was 3 times higher than that of R-HNK. When fitting the oral data of HNK and DHNK, the contribution of hepatic first-pass metabolism had to be added to achieve a reasonable fit. Although scenario 2 provided a better fit than scenario 1, the fit was still not completely satisfactory, as indicated by comparison of the observed median values with the curve simulated using the population mean values of the parameters (Figure 4).

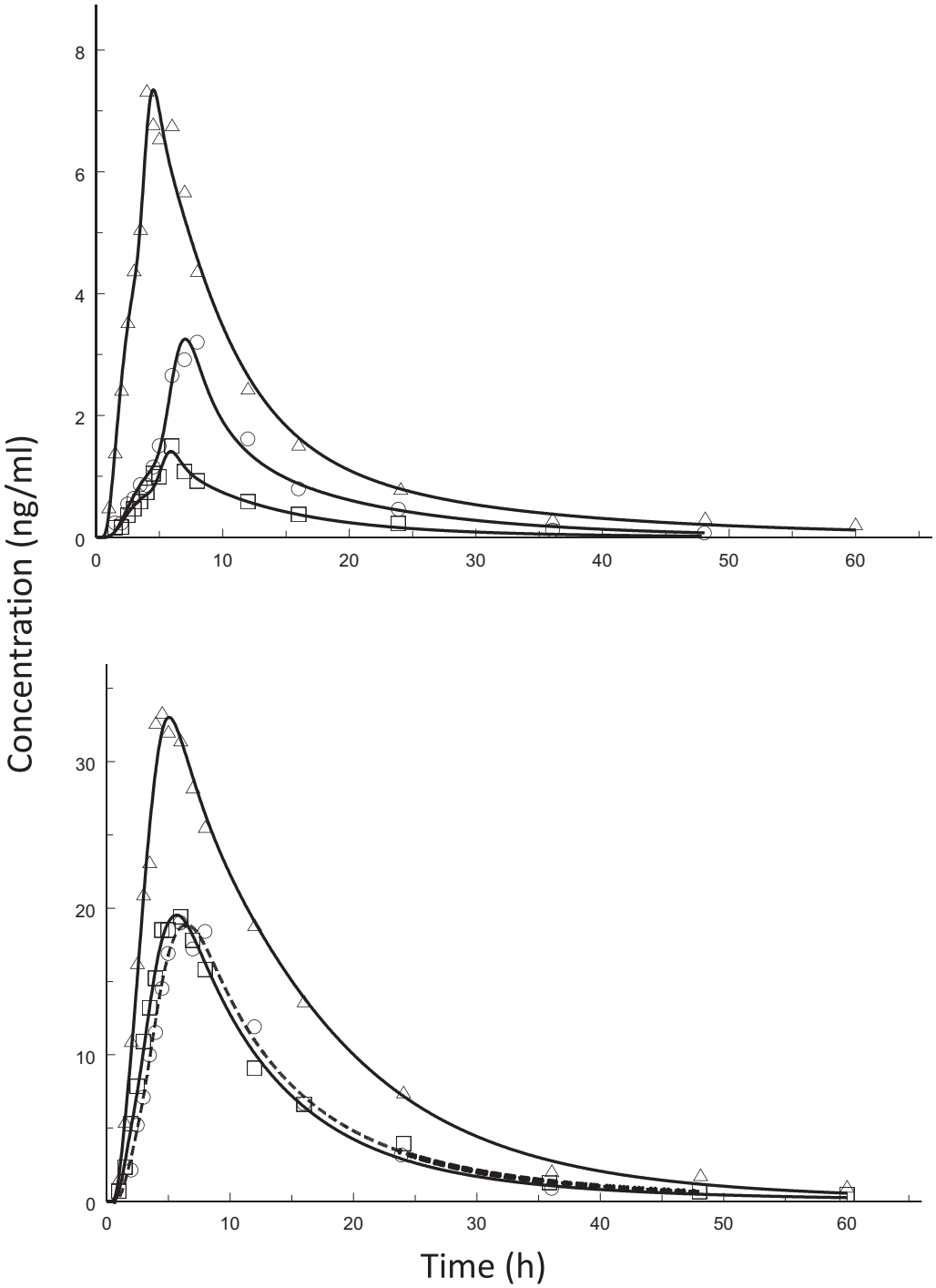

Figure 3. Top: Fits of R-ketamine data obtained after 40-mg prolonged-release ketamine tablets for 3 subjects characterized by the highest, middle, and lowest maximum concentrations, with bioavailability of 8% (open squares), 11% (open circles), and 34% (open triangles). Bottom: Fits of R-norketamine data for the same 3 subjects shown above (dashed curve for subject with bioavailability of 11%, open circles). Because of the higher hepatic extraction ratio, the concentration generated in the subject with the lowest bioavailability (open squares) increased.

One reason may be the variability in the first-pass generation of HNK and DHNK. However, it is unclear how the model could be further improved. Table 2 provides all absorption-related parameters estimated by fitting (separately) both the ketamine and NK data and then HNK and DHNK data simultaneously after 4 doses of PR-ketamine. PR-ketamine was well absorbed from the gut lumen; the low bioavailability (F) of about

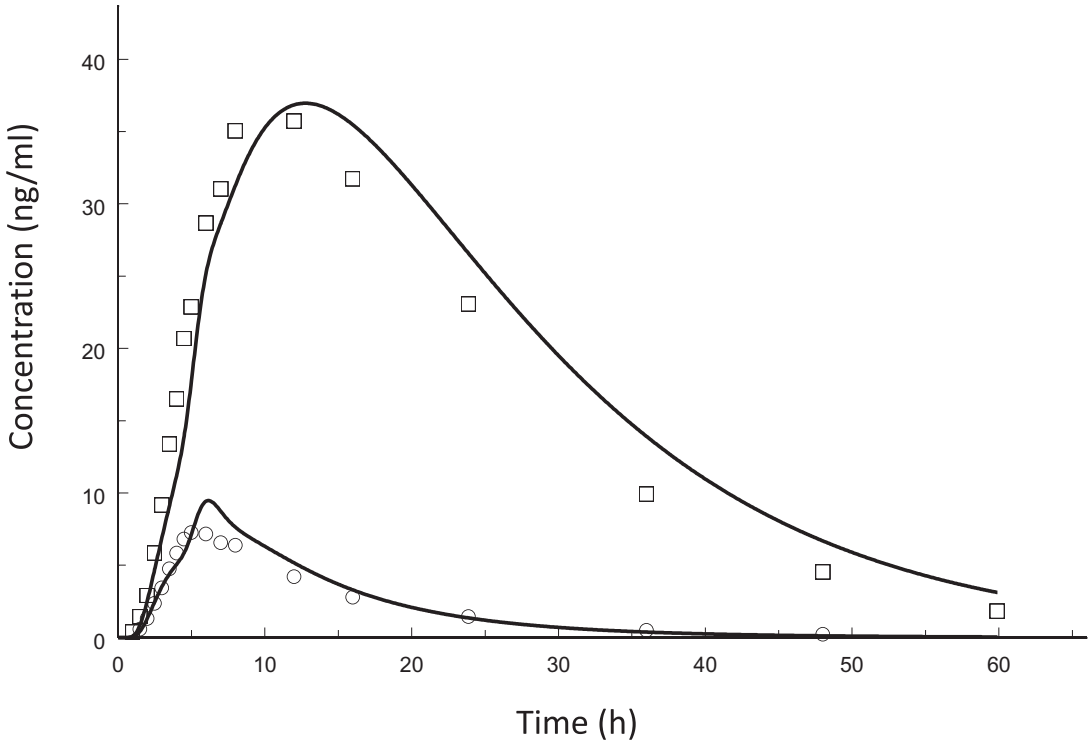

Figure 4. Model-predicted average concentration-time curves for 2R,6R-hydroxynorketamine (R-HNK) and R-dehydronorketamine (R-DHNK) after administration of 40 mg PR-ketamine, with the medians of the R-HNK data (open squares) and R-DHNK data (open circles). The curves were simulated using the population mean parameter estimates (Tables 1 and 2).

13% was because of the high first-pass extraction of approximately 80%. The fraction absorbed (F_a) appears to be lower for the S-enantiomer (significant for the 20- and 80-mg doses). For 3 of the 4 doses, the hepatic first-pass extraction of generated NK that forms HNK was significantly higher for the S-stereoisomer.

Figure 5 shows the simulated concentration-time profiles for the stereoisomers of ketamine, NK, HNK, and DHNK for a 35-mg dose of R/S-ketamine infused over 40 minutes. The corresponding simulated curves for the multiple-dose administration of PR-ketamine (20 mg twice daily) are depicted in Figure 6. All simulations were based on the population mean parameters (Tables 1 and 2). For intravenous infusion (Figure 5), a difference between the stereoisomers was found in the values of the peak serum concentrations, which were higher for R-HNK and R-DHNK compared with the S-stereoisomers. After multiple oral dosing of PR-ketamine (Figure 6), the most striking result was the high steady-state concentration of R-HNK compared with R-NK, R-DHNK, and R-ketamine. Amounting to only 3% of that of R-HNK, the concentration of R-K appeared nearly negligible. Furthermore, the average steady-state concentration of R-HNK (45.6 ng/mL) was more than 2 times higher than that of S-HNK (17.7 ng/mL) with lower fluctuations. Note that steady state was attained after about 2 days. The 90% prediction interval around the mean for the steady-state plasma concentration on R-HNK ranged from 15 to 94 ng/mL. As was expected from the intersubject variability of bioavailability, this interval was relatively wide. For the predicted maximum concentration of R-HNK after infusion, the prediction interval was smaller, ranging from 12 to 63 ng/mL.

Discussion

This is the first pharmacokinetic modeling study of ketamine enantiomers and their primary metabolites NK and distal metabolites 2,6-HNK and DHNK after oral administration of PR-ketamine tablets. The results explain the differences in metabolite exposures observed in the previous study[10] in terms of the estimated model parameters. Thus, the favored formation of R-HNK was caused by nearly 2 times higher formation clearance of R-NK and about 3 times higher elimination clearance of S-HNK compared with the respective counterpart stereoisomer.

The concentration-time curves simulated using the mean parameter estimates (Tables 1 and 2) were in perfect agreement with the medians of the observed data (Figures 2 and 4 and Supplemental Figures S3, S6, S19, and S28). There were only small deviations in Figure 4.

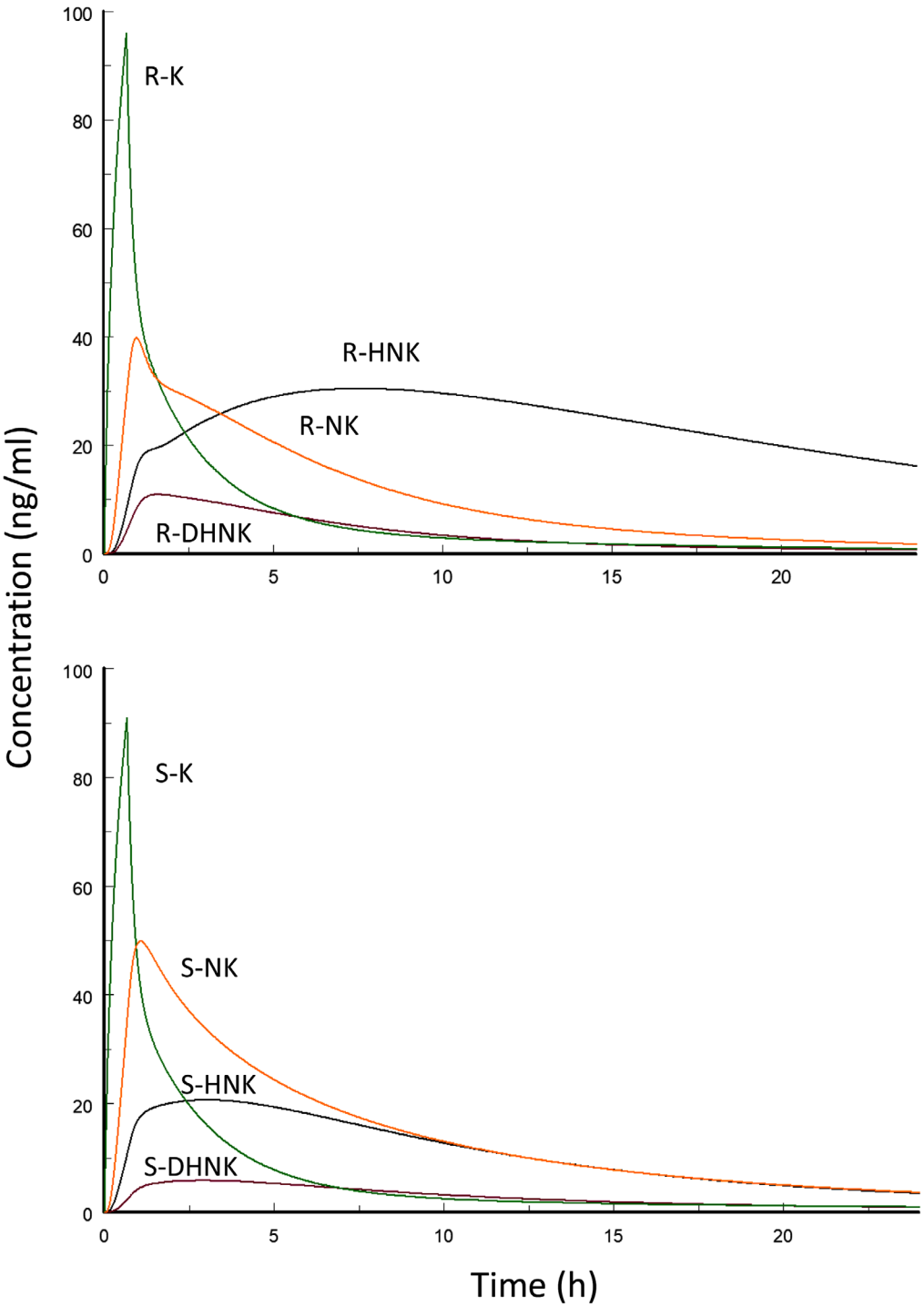

Figure 5. Simulation of plasma concentration-time profiles for a 35-mg dose of R,S-ketamine infused over 40 minutes. Top: R-ketamine (R-K), R-norketamine (R-NK), 2R,6R-hydroxynorketamine (R-HNK), and R-dehydronorketamine (R-DHNK). Bottom: S-ketamine (S-K), S-norketamine (S-NK), 2S,6S-hydroxynorketamine (S-HNK), and S-dehydronorketamine (S-DHNK). The curves were simulated using the population mean values of the parameters (Table 1).

No parameter estimates have been published so far for the secondary metabolites.[26] A previous study with intravenously administered ketamine was based on sparse data (4 times in 9 subjects).[12] Our clearance values for ketamine, $CL_{K,R}$, and $CL_{K,S}$ and the V_{ss} values were in accordance with those estimated from the present data using noncompartmental analysis[10] as well as with those reported in the literature.[27,28] Note that

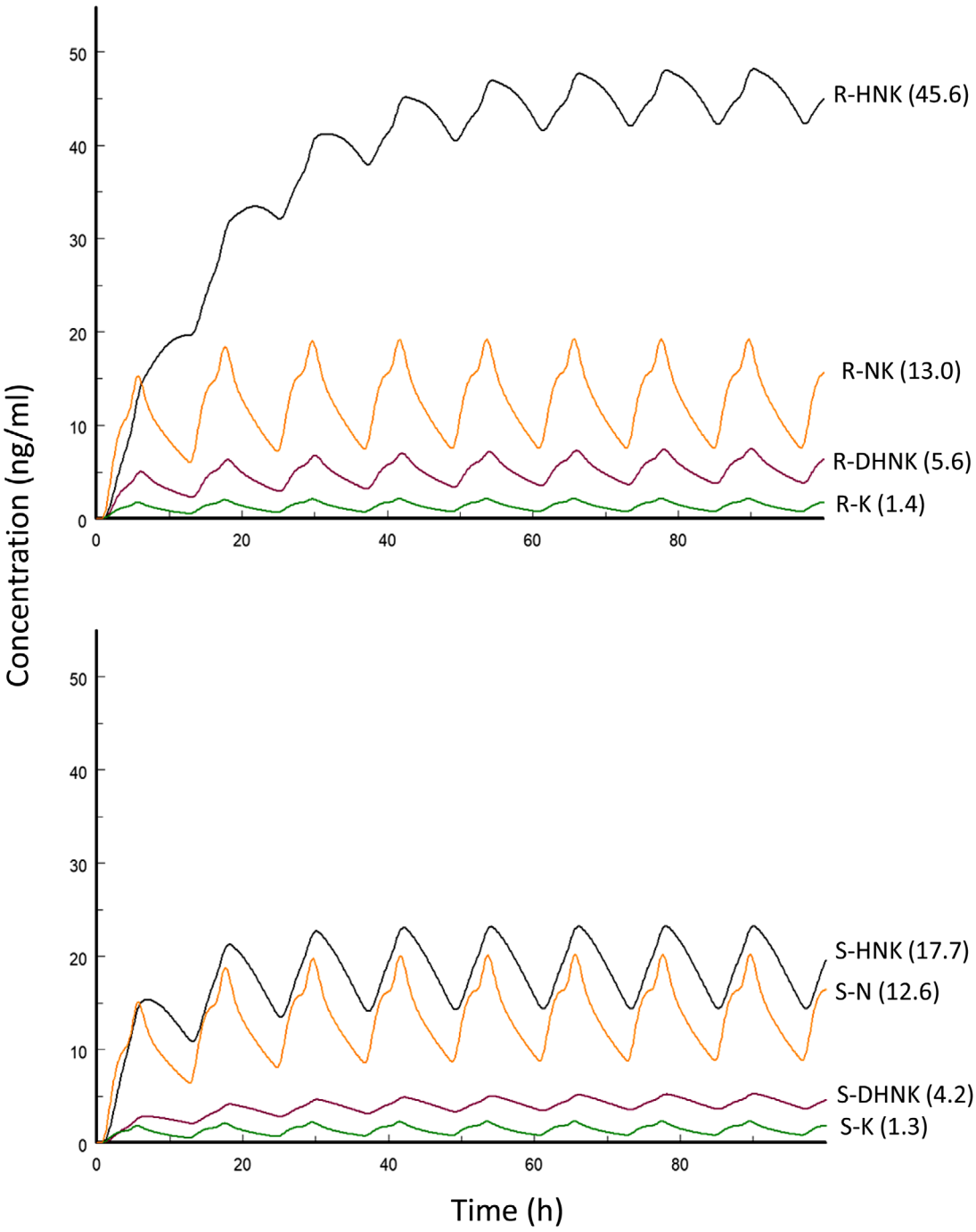

Figure 6. Simulation of plasma concentration-time profiles for multiple-dose administration of PR-ketamine (2 daily doses of 20 mg), with average steady-state concentrations in brackets. Top: R-ketamine (R-K), R-norketamine (R-NK), 2R,6R-hydroxynorketamine (R-HNK), and R-dehydronorketamine (R-DHNK). Bottom: S-ketamine (S-K), S-norketamine (S-NK), 2S,6S-hydroxynorketamine (S-HNK), and S-dehydronorketamine (S-DHNK). The curves were simulated using the population mean values of the parameters (Tables 1 and 2).

with the methods used in the study reported in the previous article,[10] renal clearance but not total clearance of metabolites could be estimated. That only the renal clearance of R-DHNK (26.4 L/h), S-DHNK (37.2 L/h), and R-HNK (1.5 L/h)[10] contributed significantly with 23%, 32%, and 21%, respectively, to their total clearance is in agreement with the more hydrophilic character of secondary metabolites. This is also reflected by their much lower distribution volumes. The distribution volume of S-NK is in agreement with that reported by

Fanta,[14] and our estimate of $CL_{NK,S}$ is somewhat lower than published values.[14,29,30] Regarding the kinetics of HNK and DHNK, only results for the racemate have been published, by Kamp et al.[13] They also reported higher clearance for DHNK compared with HNK. Notably, our results are in accordance with those reported by Zhao et al,[12] namely, the higher formation rate constants of S-DHNK compared with S-HNK, the about 2-fold-greater elimination rate constant of S-DHNK compared with S-HNK, and the higher formation rate of R-DHNK compared with S-DHNK.

The mean input time of R-and S-ketamine as well as that of R- and S-NK of about 8 hours is largely determined by the mean dissolution time (~6 hours; U.S. Patent No. 10,335,379;2019). The hepatic transit time of the generated NK (~6 minutes) after intravenous infusion is consistent with those reported previously[14,18] and determined by hepatocyte permeability.[31] Note that the hepatic transit times of ketamine and metabolites are negligible compared with their mean input times. The bioavailability of our PR-ketamine tablets of about 13% was only slightly higher than that reported for S-ketamine administered as syrup (11%),[32] but markedly higher than the 8% found by Fanta.[14] Interindividual variability was high in all cases (~50%). When fitting the HNK and DHNK data after oral administration, it became obvious that first-pass generation of these secondary metabolites has to be considered to achieve a reasonable fit. However, the interpretation of this result is uncertain. It should be taken into account that a small percentage of HNK could be formed from ketamine via 6-hydroxylation.[1] But although scenario 2 provided a slightly better fit, this does not exclude a generation of secondary metabolites from NK (scenario 1). But if extraction ratios on the order of a few percent would result from NK, the corresponding factor, F_{hNK}, would be close to 1. The significant lower extraction ratio $E_{K\text{-}HNK,R}$ for the 80-mg dose compared with the 10-mg dose suggests that the first-pass formation of R-HNK became saturated. However, in discussing the $E_{K\text{-}HNK}$ and $E_{K\text{-}DHNK}$ estimates, the high interindividual variability should also be taken into account.

Another objective of this study was the prediction of plasma concentration-time curves of ketamine and its metabolites after repeated oral-dose administration of PR-ketamine relative to intravenous infusion as currently practiced in patients with drug-resistant depression or chronic neuropathic pain.[33–35] The curves simulated for a 40-minute infusion of 35 mg of R/S-ketamine (Figure 5) are in general agreement with the data reported by Zhao et al[12]; however, because they only measured total HNK, the crucial difference between R- and S-HNK was not revealed. The concentration of generated R-HNK with a flat maximum of 30.4 ng/mL at 7.6 hours is consistent with the therapeutic level in patients with drug-resistant depression.[25] The slow decline of R-HNK concentration thereafter may explain the long duration of action observed by Berman et al.[24] That the concentration of S-HNK, in contrast, showed a maximum of 20 ng/mL at 3 hours and declined faster is because of the higher clearance. A major finding of this simulation study was the high steady-state concentration of R-HNK of about 45.6 ng/mL achieved after multiple dosing of PR-ketamine (20 mg every 12 hours; Figure 6). This concentration, reached after about 2 days, was in the therapeutic range[24,25] and was higher than the maximum concentration achieved with the 40-minute infusion (described above). The steady-state concentration of S-HNK was only half that of R-HNK and not markedly different from the S-NK concentration. Furthermore, the steady-state serum concentrations of R- and S-ketamine were negligibly low compared with the concentrations of the potential analgesic/antidepressant HNKs (~3%). These simulations may provide information to assist the design of dosage schedules. Given that R-HNK is the major potential analgesic/antidepressant component and ketamine causes NMDA-related adverse psychotropic effects, PR-ketamine tablets might be a more efficient and safer dosage form in the treatment of patients with depression and chronic neuropathic pain compared with intravenous infusion.

In summary, a compartment model has been developed and validated for the pharmacokinetic analysis of ketamine enantiomers and their downstream metabolites after administration of prolonged-release ketamine tablets. The estimated model parameters allowed the simulation of multiple dosing regimens.

Conclusions

A therapeutically efficient serum concentration of the analgesic/antidepressant 2,6-hydroxynorketamine but negligible low concentrations of the psychotropic ketamine is reached after repeated doses of 20 mg PR-ketamine given orally every 12 hours. Therefore, prolonged-release ketamine tablets can be equally efficient but safer than treatment with intravenous infusion.

Acknowledgments

The authors thank David Z. D'Argenio for his help in implementing the multiple-dose input function used in the present simulation study and Markus Grube for the multiple tests.

Open access funding enabled and organized by Projekt DEAL.

Conflicts of Interest

The authors declare no conflicts of interest.

Funding

There was no founding for our pharmacokinetic modeling of the serum concentration-time profiles of a previous clinical study (EudraCT2014-000100-10).

Data Sharing

All data analyzed in this article are filed by the University Medicine of Greifswald and can be obtained by contacting Dr. Werner Siegmund (werner.siegmund@unigreifswald.de).

References

1. Desta Z, Moaddel R, Ogburn ET, et al. Stereoselective and regiospecific hydroxylation of ketamine and norketamine. *Xenobiotica*. 2012;42(11):1076-1087.
2. Singh NS, Zarate CA Jr, Moaddel R, Bernier M, Wainer IW. What is hydroxynorketamine and what can it bring to neurotherapeutics? *Expert Rev Neurother*. 2014;14(11):1239-1242.
3. Zanos P, Moaddel R, Morris PJ, et al. Ketamine and ketamine metabolite pharmacology: insights into therapeutic mechanisms. *Pharmacol Rev*. 2018;70(3):621-660.
4. Zanos P, Moaddel R, Morris PJ, et al. NMDAR inhibition-independent antidepressant actions of ketamine metabolites. *Nature*. 2016;533(7604):481-486.
5. Kroin JS, Das V, Moric M, Buvanendran A. Efficacy of the ketamine metabolite (2R,6R)-hydroxynorketamine in mice models of pain. *Reg Anesth Pain Med*. 2019;44(1):111-117.
6. Highland JN, Zanos P, Riggs LM, et al. Hydroxynorketamines: pharmacology and potential therapeutic applications. *Pharmacol Rev*. 2021;73(2):763-791.
7. Kohtala S. Ketamine-50 years in use:from anesthesia to rapid antidepressant effects and neurobiological mechanisms. *Pharmacol Rep*. 2021;73(2):323-345.
8. McIntyre RS, Rosenblat JD, Nemeroff CB, et al. Synthesizing the evidence for ketamine and esketamine in treatment-resistant depression:an international expert opinion on the available evidence and implementation. *Am J Psychiatry*. 2021;178:383-399.
9. Glue P, Medlicott NJ, Neehoff S, et al. Safety and efficacy of extended release ketamine tablets in patients with treatment-resistant depression and anxiety: open label pilot study. *Ther Adv Psychopharmacol*. 2020;10:2045125320922474.1–6.
10. Hasan M, Modess C, Roustom T, et al. Chiral pharmacokinetics and metabolite profile of prolonged-release ketamine tablets in healthy human subjects. *Anesthesiology*. 2021;135:326-339.
11. Weiss M. Empirical models for fitting of oral concentration time curves with and without an intravenous reference. *J Pharmacokinet Pharmacodyn*. 2017;44(3):193-201.
12. Zhao X, Venkata SL, Moaddel R, et al. Simultaneous population pharmacokinetic modelling of ketamine and three major metabolites in patients with treatment-resistant bipolar depression. *Br J Clin Pharmacol*. 2012;74(2):304-314.
13. Kamp J, Jonkman K, van Velzen M, et al. Pharmacokinetics of ketamine and its major metabolites norketamine, hydroxynorketamine, and dehydronorketamine: a model-based analysis. *Br J Anaesth*. 2020;125(5):750-761.
14. Fanta S, Kinnunen M, Backman JT, Kalso E. Population pharmacokinetics of S-ketamine and norketamine in healthy volunteers after intravenous and oral dosing. *Eur J Clin Pharmacol*. 2015;71(4):441-447.
15. Ashraf MW, Peltoniemi MA, Olkkola KT, Neuvonen PJ, Saari TI. Semimechanistic population pharmacokinetic model to predict the drug-drug interaction between s-ketamine and ticlopidine in healthy human volunteers. *CPT Pharmacometrics Syst Pharmacol*. 2018;7(10):687-697.
16. Fassauer GM, Hofstetter R, Hasan M, et al. Ketamine metabolites with antidepressant effects: fast, economical, and eco-friendly enantioselective separation based on supercritical-fluid chromatography (SFC) and single quadrupole MS detection. *J Pharm Biomed Anal*. 2017;146:410-419.
17. Hasan M, Hofstetter R, Fassauer GM, Link A, Siegmund W, Oswald S. Quantitative chiral and achiral determination of ketamine and its metabolites by LC-MS/MS in human serum, urine and fecal samples. *J Pharm Biomed Anal*. 2017;139:87-97.
18. Herd DW, Anderson BJ, Holford NH. Modeling the norketamine metabolite in children and the implications for analgesia. *Paediatr Anaesth*. 2007;17(9):831-840.
19. Weiss M. A general model of metabolite kinetics following intravenous and oral administration of the parent drug. *Biopharm Drug Dispos*. 1988;9(2):159-176.
20. Csajka C, Drover D, Verotta D. The use of a sum of inverse Gaussian functions to describe the absorption profile of drugs exhibiting complex absorption. *Pharm Res*. 2005;22(8):1227-1235.
21. Wendling T, Ogungbenro K, Pigeolet E, Dumitras S, Woessner R, Aarons L. Model-based evaluation of the impact of formulation and food intake on the complex oral absorption of mavoglurant in healthy subjects. *Pharm Res*. 2015;32(5):1764-1778.
22. Weiss M. A novel extravascular input function for the assessment of drug absorption in bioavailability studies. *Pharm Res*. 1996;13(10):1547-1553.
23. D'Argenio DZ, Schumitzky A, Wang X. *ADAPT 5 user's guide: Pharmacokinetic/pharmacodynamic systems analysis software*. Los Angeles, CA: Biomedical Simulations Resource; 2009.

24. Berman RM, Cappiello A, Anand A, et al. Antidepressant effects of ketamine in depressed patients. *Biol Psychiatry*. 2000;47(4):351-354.
25. Zarate CA, Jr., Brutsche N, Laje G, et al. Relationship of ketamine's plasma metabolites with response, diagnosis, and side effects in major depression. *Biol Psychiatry*. 2012;72(4):331-338.
26. Kamp J, Olofsen E, Henthorn TK, et al. Ketamine Pharmacokinetics. *Anesthesiology*. 2020;133(6):1192-1213.
27. Geisslinger G, Hering W, Kamp HD, Vollmers KO. Pharmacokinetics of ketamine enantiomers. *Br J Anaesth*. 1995;75(4):506-507.
28. Henthorn TK, Avram MJ, Dahan A, et al. Combined Recirculatory-compartmental population pharmacokinetic modeling of arterial and venous plasma S(+) and R(-) ketamine concentrations. *Anesthesiology*. 2018;129(2):260-270.
29. Noppers I, Olofsen E, Niesters M, et al. Effect of rifampicin on S-ketamine and S-norketamine plasma concentrations in healthy volunteers after intravenous S-ketamine administration. *Anesthesiology*. 2011;114(6):1435-1445.
30. Sigtermans M, Dahan A, Mooren R, et al. S(+)-ketamine effect on experimental pain and cardiac output: a population pharmacokinetic-pharmacodynamic modeling study in healthy volunteers. *Anesthesiology*. 2009;111(4):892-903.
31. Mellick GD, Anissimov YG, Bracken AJ, Roberts MS. Metabolite mean transit times in the liver as predicted by various models of hepatic elimination. *J Pharmacokinet Biopharm*. 1997;25(4):477-505.
32. Peltoniemi MA, Saari TI, Hagelberg NM, et al. Rifampicin has a profound effect on the pharmacokinetics of oral S-ketamine and less on intravenous S-ketamine. *Basic Clin Pharmacol Toxicol*. 2012;111(5):325-332.
33. Diazgranados N, Ibrahim L, Brutsche NE, et al. A randomized add-on trial of an N-methyl-D-aspartate antagonist in treatment-resistant bipolar depression. *Arch Gen Psychiatry*. 2010;67(8):793-802.
34. Kamp J, Van Velzen M, Olofsen E, Boon M, Dahan A, Niesters M. Pharmacokinetic and pharmacodynamic considerations for NMDA-receptor antagonist ketamine in the treatment of chronic neuropathic pain: an update of the most recent literature. *Expert Opin Drug Metab Toxicol*. 2019;15(12):1033-1041.
35. Zarate CA Jr, Brutsche NE, Ibrahim L, et al. Replication of ketamine's antidepressant efficacy in bipolar depression: a randomized controlled add-on trial. *Biol Psychiatry*. 2012;71(11):939-946.

Supplemental Information

Additional supplemental information can be found by clicking the Supplements link in the PDF toolbar or the Supplemental Information section at the end of web-based version of this article.